Journal of Physical Chemistry and Functional Materials

Home Page of Journal: https://dergipark.org.tr/jphcfum

Response Surface Methodology Optimized Eriochrome Black T Dye Removal Using Alumina Beads: Isotherms and Kinetics Studies

Abdu Muhammad Bello*, Abubakar Hamisu, Naziru Alhassan Muhammad

Department of Chemistry, Faculty of Sciences, Kano University of Science and Technology Wudil, PMB 3244, Kano State, Nigeria

**Corresponding author:* Abdu Muhammad Bello *E-mail: muhbaf70@yahoo.com*

ABSTRACT

Numerous approaches have been investigated to develop cheaper and more effective technologies toward improving the quality of industrial effluent. However, adsorption has been one of the most simplest and economical remediation technology in the treatment of wastewaters. In this study, commercial alumina beads (Al-beads) were utilized for the adsorption of Eriochrome Black T dye. The adsorption process was optimized using the RSM model by Central Composite Design. The optimization result reveals the most influential variables as; the adsorbent dosage, initial dye concentration, interaction between adsorbent dosage with itself, interaction of pH with itself, and that of adsorbent dosage with initial dye concentration. The R^2 value of 0.9314 implies that 93.14% of the percent dye removal could be due to the variation in the independent variable. Whereas the Adeq. precision of 13.130, and lack of fit (3.13) signifies the model can be used to navigate the design space. Up to 98.28%, dye removal was attained using the Al-beads under the conditions; pH of 12.39, adsorbent dosage (1.25 g), and initial dye concentration (175 ppm). The adsorption data indicated that the adsorption process was fitted to Freundlich and Temkin isotherm models, while for the kinetics study, the pseudo-second-order model was the best fit. Furthermore, the adsorption mechanism was found to be governed majorly by intra-particle diffusion with some contribution from external mass transfer diffusion.

ARTICLE INFO

Keywords:
Alumina beads
Echanism
RSM
Eriochrome Black T.

Received: 2022-03-30
Accepted: 2022-05-25
ISSN: 2651-3080
DOI: 10.54565/jphcfum.1095968

1. Introduction

Ever since man progressed from hunting to agriculture, with the subsequent establishment of stable communities, the problem of water pollution has been his main concern. This is because alongside this growth, is the generation of waste material and the associated problem of disposal [1]. The main concern with water pollution is its transboundary nature. Thus, water contamination is a major international problem caused by industrial, domestic, and environmental influences, as such water-related problems are a persistent global issue. Various factors, such as population growth, urbanization, and industrialization, have continually stressed hydrological resources. The lack of wastewater management, and the poor public policies, make the situation worse [2].

Textile, paper, printing, and dye industries are the major sources of contamination responsible for the incessant environmental pollution due to the excessive release of natural and synthetic dyes. They produced about 7 x 10^5 tonnes of dyes and pigments yearly, and out of this 1 to 15% is lost in the effluents. These organic chemicals find their way into the waterways, posing aesthetic concerns and promoting eutrophication. They are also carcinogenic, mutagenic, allergenic, and toxic nature [3].

Additionally, the dye-containing effluents are colored, and highly visible making the water objectionable. Furthermore, the effluents are very difficult to treat due to the synthetic-origin complex nature of the dyes. They are resistant to aerobic digestion and are stable to light, heat, and oxidizing agents. Among these dyes, water-soluble and brightly colored acid and reactive dyes are the most challenging, as they tend to pass through conventional decolorization systems unaffected [4, 5].

Several contamination response techniques; filters, chemical dosing, reverse osmosis, gravity separation, ultra-filtration, micro-filtration, biological processes, air flotation, membrane bioreactor, chemical coagulation, electro-coagulation, and electro-flotation, have been investigated for wastewater remediation. However, adsorption has been proven to be superior for wastewater treatment in terms of economy, flexibility and simplicity of design, ease of operation, insensitivity to toxic pollutants, and does not produce harmful substances [6–9]. Many adsorbents have been developed for the treatment of the effluents of textile industries.

Alumina due to its physical, textural, thermal, and chemical properties, has found a wide range of applications in catalytic and separation processes, host-guest chemistry, adsorbent host for quantum structures, separation of large biological molecules, and environmental pollution control. The pore structural properties of alumina, high surface area, and large pore volume allow for higher adsorption of pollutants. Thus, alumina (Al_2O_3) beads with a large surface area can be an excellent adsorbent for the remediation of industrial wastewater. Additionally, since the alumina beads are in granular form, the separation of the adsorbent from the adsorbate will be much easier after the adsorption, which is one of the requirements of any industrial process. In this study alumina beads with a specific surface area of 93 m^2/g were employed for the remediation of Eriochrome Black T dye contaminated wastewater.

One-variable-at-a-time (OVAT) method has been generally employed for the optimization of the adsorption process. However, this method cannot illustrate the complete effects of all variables on the response. This is because only one variable is varied at a time keeping other variables constant. Furthermore, many experimental runs are required to optimize the parameters making it time-consuming and expensive. Thus, multivariate statistical techniques have been introduced, and the most relevant of these techniques is response surface methodology (RSM). RSM is a set of mathematical and statistical techniques that describe the behaviour of a data set based on the fit of the polynomial equation to the experimental data to make a statistical prediction. It has the advantage of simultaneously optimizing all variables to obtain the response [10]. This study employed the Central Composite Design model for the optimization of the dye removal process.

2. Experimental

2.1 Materials

The hydrochloric acid and sodium hydroxide were purchased from QRëC™. While the Eriochrome Black T (EBT) dye and commercial alumina beads (Al-beads) were supplied by Sigma Aldrich. All reagents were of analytical grade and used without further purification.

2.2 Batch Adsorption Study

The adsorption process was performed in a plastic sample bottle by collecting 100 mL of specific dye concentration,

and adjusting the pH using 0.1 M solutions of NaOH and HCl, then adding a definite amount of the Al-beads adsorbent, followed by shaking on a mechanical shaker for 30 minutes. At the end of the experiment, the dye solution was separated using Whatman No 42 filter paper and the absorbance was monitored using a Perkin Elmer UV-Visible spectrophotometer (Perkin Lambda) at a wavelength of 530 nm.

2.3 Statistical Analysis and Model Fitting

The adsorption experiments were optimized using response surface methodology (RSM) analysis applying three-level factorial Central Composite Designs. The design factors are; adsorbent dosage, initial dye concentration, and pH. Design-Expert 7.0 software was employed for the analysis. For predicting the optimal point after performing experiments, a second-order polynomial quadratic equation (Equation 1) was fitted to correlate the relationship between independent variables and responses and the interactive effect of the process variables. Regression coefficients of the quadratic model were evaluated by analysis of variance (ANOVA). All the terms in the model were tested by the student's F-test and the significance of the F-values at probability levels ($p \leq 0.05$) was analyzed. The developed mathematical models were used for the construction of three-dimensional (3D) response surface plots to predict the relationships between independent and dependent variables. The experimental data were evaluated with a determination coefficient (R^2), adjusted determination of coefficient (R^2 adj.), and predicted determination of coefficient (R^2 pred.). Verification experiments were performed under the optimal conditions and the values of the experiments were compared with the predicted values of the developed model equations.

$$Y = \lambda_o + \sum_{i=1}^{k} \lambda_i x_i + \sum_{i=1}^{k} \lambda_{ii} x_i^2 + \sum_{i=1}^{k} \sum_{j=i+1}^{k} \lambda_{ij} x_i x_j + \varepsilon$$

Where Y is the response, i and j are the linear and quadratic coefficients, respectively, k is the number of the studied and optimized factors in the experiment, λ is the regression coefficient, and ε is the arbitrary error [11].

The amount of EBT dye uptake by Al-beads was calculated using Equation 2;

$$q_e = \frac{(Co - Ce)V}{W} \ldots\ldots 2$$

Where, C_o is the initial concentration of adsorbate (mg/L), C_e is the final concentration of adsorbate (mg/L), W is the mass of adsorbent in gram (g), V is the volume of the adsorbate in a liter (L), and q_e is the adsorption capacity.

The adsorption efficiency can be expressed as the percentage removal of dye solution using Equation 3;

$$\text{Dye removal}\,(\%) = \frac{(Co - Ce)}{Co} x\,100 \ldots\ldots 3$$

3 Results And Discussion

3.1 Response Surface Methodology

Three-level factorial Central Composite Design was applied for the RSM analysis, and the design factors were: Adsorbent dosage (g); A (0.5-2 g), Initial dye concentration; B (50-300 ppm), and pH; C (3-10). From the regression surface analysis and the analysis of variance (ANOVA), the second-order polynomial equation in terms of actual factors obtained from the multiple regression analysis of the experimental data for the Al-beads is expressed in Equations 4;

$$Y = 62.82668 - 7.05543 \times A - 12.80112 \times B + 0.022598 \times C - 14.35875 \times A \times B - 0.99625 \times A \times C + 3.39125 \times B \times C - 9.81560 \times A^2 + 4.65181 \times B^2 + 11.72287 \times C^2 \ldots\ldots 4$$

Where, Y is the response (i.e. % dye removal), and A, B, and C are the actual factors of the studied variables.

Table 1 depicts the actual values of the adsorption parameters and the responses obtained from the experiments conducted, as well as the predicted responses. While Table 2 is the result of ANOVA from the fitting of the experimental data to a second-order response surface model.

The model reveals that A, B, A^2, C^2, and AB are the significant model terms. Thus, the most influential variables are the adsorbent dosage, initial dye concentration, the interaction between adsorbent dosage with itself, the interaction between pH with itself, and that of adsorbent dosage with initial dye concentration. This is clear from Figure 1 where the 3D graphical representation of the effect of interaction between the three variables (adsorbent dosage, initial dye concentration, and pH) on the percent dye removal is depicted. The fact that the adsorbent dosage and

initial dye concentration, as well as their interaction, are among the significant model's terms, may be explained by the observation that pH has the least effect on the percent dye removal. This is because the percent dye removal is efficient both in an acidic and alkaline medium. This can be the reason for the interaction of pH with itself being among the most influential model terms.

It can be observed from Figure 1a that there is positive interaction between adsorbent dosage and initial dye concentration, i.e. the percent dye removal increased with the increase of the two variables. Figure 1b shows the interaction between adsorbent dosage and pH, from it the pH was observed to increase then decreased and again increased, this explains the initial assertion that the percent dye removal is effective in acidic and alkaline conditions, but low in the neutral condition. Finally, Figure 1c depicted the interaction of initial dye concentration with pH, the percent dye removal was observed to decrease with initial dye concentration, but increased initially with pH, slightly decreased, and finally increased.

Table 1: Three-level factorial Box-Behnken Design and the response

Std	Run	Block	Factor 1 A: Adsorbent Dosage (g)	Factor 2 B: Initial Concn. (ppm)	Factor 3 C: pH	Response 1 Percent Dye Removal (%)	Predicted Percent Dye Removal (%)
14	1	Block 1	1.25	175.00	12.39	98.28	96.02
7	2	Block 1	0.50	300.00	10.00	83.42	82.41
8	3	Block 1	2.00	300.00	10.00	32	37.59
4	4	Block 1	2.00	300.00	3.00	39.42	32.75
9	5	Block 1	0.01	175.00	6.50	55.42	46.93
5	6	Block 1	0.50	50.00	10.00	63.00	72.51
20	7	Block 1	1.25	175.00	6.50	56.00	62.83
11	8	Block 1	1.25	35.22	6.50	97.71	97.51
19	9	Block 1	1.25	175.00	6.50	66.00	62.83
12	10	Block 1	1.25	385.22	6.50	58.28	54.46
15	11	Block 1	1.25	175.00	6.50	68.99	62.83
17	12	Block 1	1.25	175.00	6.50	55.60	62.83
3	13	Block 1	0.50	300.00	3.00	62.76	73.59
18	14	Block 1	1.25	175.00	6.50	65.14	62.83
1	15	lock 1	0.50	50.00	3.00	80.00	77.26
6	16	Block 1	2.00	50.00	10.00	93.11	85.13
2	17	Block 1	2.00	50.00	3.00	90.00	93.86
13	18	Block 1	1.25	175.00	0.61	97.71	95.95

10	19	Block 1	2.51	175.00	6.50	18.73	23.20	
16	20	Block 1	1.25	175.00	6.50	64.54	62.83	

Table 2: Analysis of variance (ANOVA) for the quadratic model

Source of Variation	Quadratic Sum of Squares	Model Degree of Freedom (df)	Mean Square	F-Values	P-Values Prob>F	Remarks
Model	8696.65	9	966.29	15.08	0.0001	Significant
A	679.83	1	679.83	10.61	0.0086	
B	2237.93	1	2237.93	34.93	0.0001	
C	6.974E-003	1	6.974E-003	1.089E-004	0.9919	
A^2	1388.47	1	1388.47	21.67	0.0009	
B^2	311.85	1	311.85	4.87	0.0519	
C^2	1980.48	1	1980.48	30.91	0.0002	
AB	1649.39	1	1649.39	25.74	0.0005	
AC	7.94	1	7.94	0.12	0.7321	
BC	92.00	1	92.00	1.44	*0.2584*	
Residual	640.67	10	640.67			
Lack of Fit	485.58	5	97.12	3.13	0.1180	not significant
Pure error	155.09	5	31.02			
Cor Total	9337.32	19				

Generally, the percentage EBT removal by the Al-beads is observed to increase with adsorbent dosage, then drop. This is attributed to the increase in the number of active sites for dye adsorption with a corresponding increase in adsorbent amount. Subsequently, as the adsorbent amount increases, the adsorption process slows down due to the overlap of active sorption sites resulting in the lowering of total available active sorption sites. Further increase in the adsorbent dosage, appeared to congest the solution, resulting in the drop off of the dye adsorption [12].

The result also shows that the adsorption varies with the initial dye concentrations, depending on the remaining two parameters. With an increase in the initial dye concentration, the percent EBT removal increases until the optimum concentration is reached, and any further increase in the initial dye concentration results in a decline in the percent dye removal. This may be attributed to the fact that the active sorption sites on the Al-beads surface were saturated with adsorbed EBT at high initial dye concentrations.

The pH of the system is an important variable for the adsorption process, it determines the surface charge of the adsorbent and the state of adsorbate in solution. The result of

the adsorption of EBT onto the Al-beads shows that the sorption is favoured both under acidic and alkaline conditions, signifying the amphoteric nature of the adsorbent. Whereas, percent dye removal is generally lower near a neutral pH. Consequently, the highest percent dye removal of 98.28% was obtained under the conditions; 1.25 g adsorbent dosage, 175 ppm initial dye concentration, and a pH of 12.39.

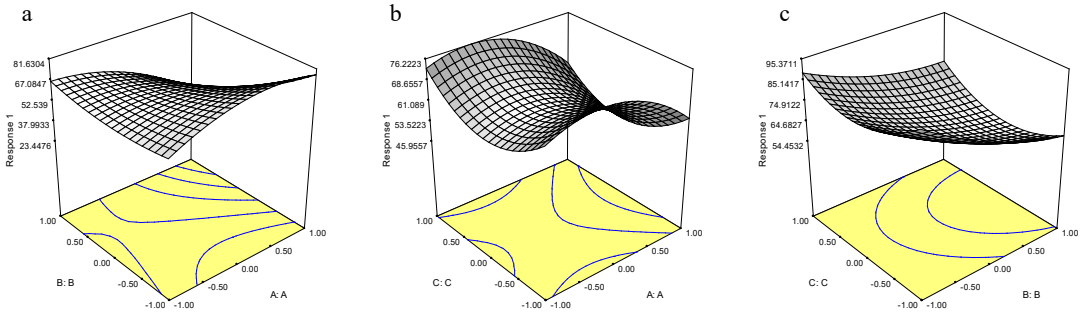

Figure 1: Interaction between a. initial dye concentration and adsorbent dosage, b. pH and adsorbent dosage, and c. pH and initial dye concentration

3.2 Validation of the Model

To validate the model and prove its fitness for predicting EBT dye removal, the predicted and experimental percent dye removal were compared in Table 1. Accordingly, there is a very good agreement between the predicted and experimental values. For instance, the first experimental run revealed a predicted percent dye removal of 96.02%, and when the experiment was run a removal of 98.28% was obtained, similarly to the remaining runs. Furthermore, the model reveals an R^2 value of 0.9314, indicating 93.14% of the effect on percent dye removal could be due to the variation in the independent variables and the remaining 6.86% is the residue. Also, the Adeq. Precision value of 13.130 in this model indicates an adequate signal, which implies that the model can be used to navigate the design space. While the "Lack of Fit F-value" of 3.13 implies it is not significant relative to the pure error, and there is an 11.80% chance that a "Lack of Fit F-value" this large could occur due to noise. This further validates the model's fit.

3.3 Mechanisms for EBT Removal at Different pH_{pzc}

The adsorption process principally relies on the zero point charge (ZPC) of an adsorbent, which is the pH at which a solid submerged in an electrolyte exhibits zero net electrical charge on the surface. Typically, the ZPC for alumina fall within the range of pH 8–10, depending on the grades [13]. The alumina surface is negatively charged at pH > pH_{ZPC}, positively charged at pH < pH_{ZPC}, and neutral at pH = pH_{ZPC}. Thus, the mechanism of the Al-beads in EBT removal at different pH_{pzc} could most probably proceed as follows:

At pH > pH_{PZC}: the mechanism for the dye removal could be expressed as in Equations 5-7;

$$Al(OH)_4^- + 3C_{20}H_{12}N_3O_7S^- \rightarrow Al(OH)(C_{20}H_{12}N_3O_7S^-)_3 + 3OH^- \ldots\ldots 5$$

$$Al(OH)_4^- + 2C_{20}H_{12}N_3O_7S^- \rightarrow Al(OH)_2(C_{20}H_{12}N_3O_7S^-)_2 + 2OH^- \ldots\ldots 6$$

$$Al(OH)_4^- + C_{20}H_{12}N_3O_7S^- \rightarrow Al(OH)_3C_{20}H_{12}N_3O_7S^- + OH^- \ldots\ldots 7$$

At pH = pH_{PZC}: the removal of EBT would be according to Equation 8

$$Al(OH)_3 + 3C_{20}H_{12}N_3O_7S^- \rightarrow Al(C_{20}H_{12}N_3O_7S^-)_3 + 3OH^- \ldots\ldots 8$$

At pH < pH_{PZC}: the Al-beads surface become positively charged as expressed in Equations 9.

$$Al(OH)_3 + H^+ \rightarrow Al(OH)_2^+ + H_2O \ldots\ldots 9$$

Subsequently, the EBT would adhere to the positive charge surface according to Equation 10.

$$Al(OH)_2^+ + 3C_{20}H_{12}N_3O_7S^- \rightarrow Al(C_{20}H_{12}N_3O_7S^-Na)_3 + 2OH^- \ldots\ldots 10$$

3.4 Adsorption Isotherm

The EBT adsorption onto the Al-beads at equilibrium relative to the equilibrium concentration was studied using Langmuir, Freundlich, and Temkin isotherms models. The Langmuir isotherm considers monolayer adsorption of adsorbate onto a homogeneous sorbent surface, while the Freundlich isotherm allows for multilayer adsorption onto a heterogeneous surface. On the other hand, the Temkin isotherm model takes into account the interactions between adsorbate and adsorbent species [14]. The Langmuir isotherm is given in Equation 11:

$$q_e = \frac{q_m K_L C_e}{1 - K_L C_e} \ldots\ldots 11$$

Where q_e is the adsorption capacity (mg/g), q_m is q_e for a complete monolayer (mg/g), C_e is the equilibrium concentration (mg/L) and K_L is the adsorption equilibrium constant (L/mg) [14, 15]. The linear form of the Langmuir isotherm in Equation 12 was used for appraising the applicability of the Langmuir isotherm to the adsorption data [17].

$$\frac{C_e}{q_e} = \frac{1}{q_m} C_e + \frac{1}{K_L q_m} \ldots\ldots 12$$

The plot of C_e/q_e against C_e in Figure 1 indicated a non-linear plot, implying the data did not fit to Langmuir model.

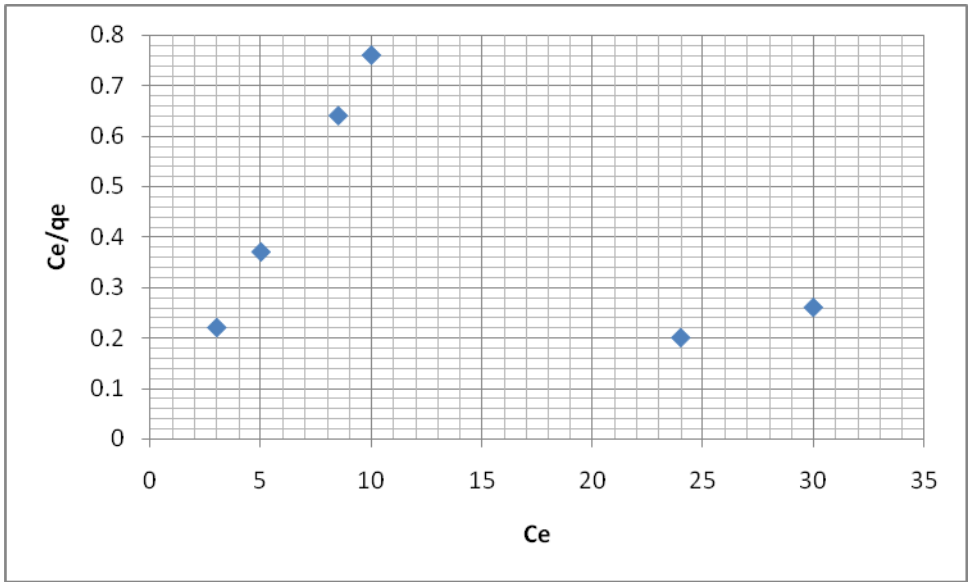

Figure 1: Langmuir isotherm plot

The possibility of multisite adsorption of EBT onto Al-beads surface was then evaluated using the Freundlich isotherm expression in Equation 13 [17].

$$\log q_e = \log K_F + \frac{1}{n} \log C_e \ldots\ldots 13$$

Where K_F and n are Freundlich constants that stand for the adsorption capacity and heterogeneity factor, respectively, their values depend on experimental conditions. If the value of $1/n$ is less than 1, the adsorbent is heterogeneous [11, 17]. The plot of log q_e against log C_e in Figure 2 gives a straight line with high correlation coefficients of 0.910, and K_F value

of 15.35. The value of $1/n = 0.075$ ($1/n < 1$), equivalent to n = 13.33 (n > 1). indicates the adsorbent is heterogeneous and suggests favorable adsorption [16]. Thus, Freundlich isotherm is considered fit for the adsorption data. Hence, there is multilayer adsorption onto a heterogeneous surface [12].

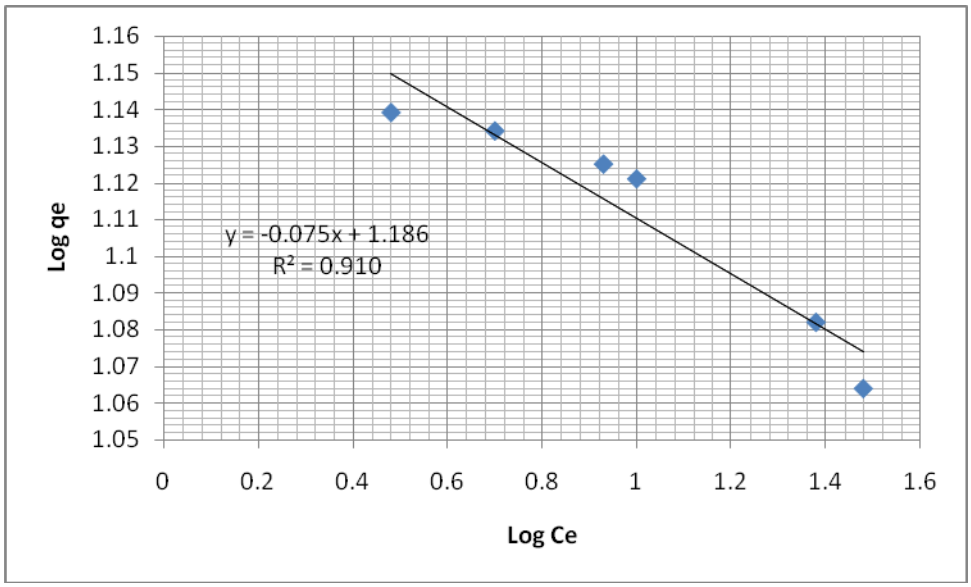

Figure 2: Freundlich isotherm plot

Finally, the linear form of the Temkin model expressed in Equation 14 was also tested for the model's fit.

$$q_e = B \ln K_T + B \ln C_e \ldots\ldots 14$$

And,

$$B = \frac{RT}{b}$$

Where; K_T is the Temkin equilibrium binding constant (L/mg) corresponding to maximum binding energy, and constant B is related to the heat of adsorption [19]. The Tempkin equation assumes that the heat of adsorption of all the molecules in the layer would decrease linearly with the coverage involved in the adsorbent–adsorbate interactions, and the adsorption is characterized by a uniform distribution of binding energies, up to some maximum energy [20]. A plot of q_e versus ln C_e in Figure 3 yields a straight line with high correlation coefficients of 0.920, which suggests this model also satisfied the experimental data. Table 3 presents the summary of the isotherms models' parameters for the adsorption data.

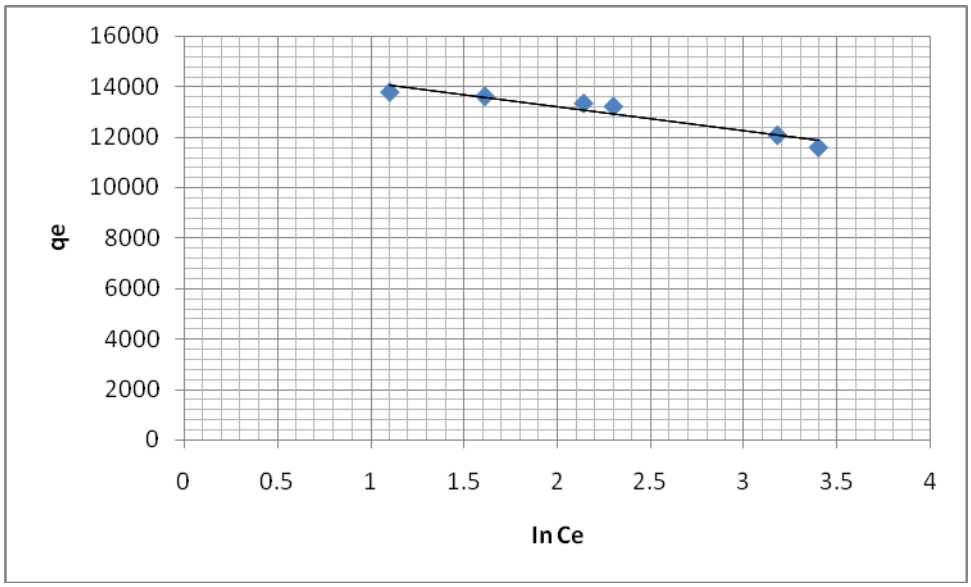

Figure 3: Temkin isotherm plot

Table 3: Adsorption isotherms models' parameters

Freundlich adsorption isotherm	
K_F (L mg^{-1})	15.35
N	13.33
R^2	0.910
Temkin adsorption isotherm	
K_T (L mg^{-1})	7.96
B	0.95
R^2	0.920

3.5 Adsorption Kinetics

The Lagergren pseudo-first-order and the pseudo-second-order models are used to evaluate the kinetic order of the adsorption process. The pseudo-first-order expression is given in Equation 15:

$$\frac{dq_t}{dt} = k_1(q_e - q_t) \ldots\ldots 15$$

Where, q_t (mg/g) is the dye concentration at any time t, q_e (mg/g) is the maximum sorption capacity, and k_1 (min^{-1}) is the rate constant [15]. On integration, the linear form in Equation 16 is obtained.

$$\log(q_e - q_t) = -\frac{k_1}{2.303}t + \log q_e \ldots\ldots 16$$

The values of k_1, and q_e can be obtained from the slope and intercept of the linear plot of log (q_e - q_t) against t. Conversely, the pseudo-first-order plot was a scatter; hence, the adsorption data does not fit this kinetics model.

Consequently, the pseudo-second-order kinetics model expression in Equation 17 was tested for the model fit.

$$\frac{dq_t}{dt} = k_2(q_e - q_t)^2 \ldots\ldots 17$$

Where, q_t (mg/g) is the dye concentration at any time t, q_e (mg/g) is the maximum sorption capacity and k_2 (g mg^{-1} min^{-1}) is the rate constant [15]. The linear form of the pseudo-second-order in Equation 18 is used for the model testing.

$$\frac{t}{q_t} = \frac{1}{k_2 q_e^2} + \frac{t}{q_e} \ldots\ldots 18$$

The plot of t/q_t against time t gives a straight line (Figure 4), with an R^2 value of 0.989. The high R^2 value indicates that the pseudo-second-order model suitably fits the kinetics model. The pseudo-second-order model has been reported as the most appropriate for describing ionic-type adsorption. This means the EBT adsorption onto Al-beads is chemisorption in nature. The finding is further substantiated by the agreement between the calculated and the experimental q_e of 11.36 mg/g and 13.76 mg/g, respectively [13]. Table 4 presents the summary of the kinetics model's constants that fitted the adsorption data.

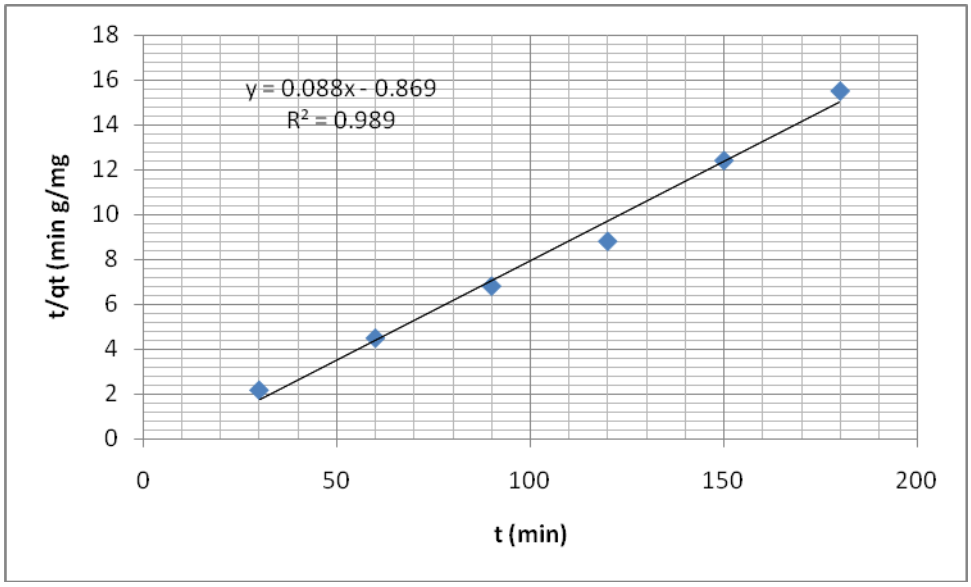

Figure 4: Pseudo-second-order plot

Table 4: Adsorption kinetics model constant and correlation coefficient

Pseudo-second-order model	
q_e, cal (mg g^{-1})	11.36
k_2 (g mg^{-1} min^{-1})	0.0089
R^2	0.989

Furthermore, the maximum adsorption capacity obtained for Al-beads obtained in this study is compared with the q_{max} for other adsorbents in the literature in Table 5. It is glaring that the q_{max} for the Al-beads in this study is similar to that of mesoporous alumina reported in [13], probably due to similarities in their properties.

Table 5: Comparison of the maximum adsorption with the literature values

Adsorbents	q_{max} (mg g^{-1})	Reference
Al-beads	13.76	This study
Soil	68.42	[21]
Activated carbon	552	[22]
Nickel oxide nanocatalyst	56.24	[6]
Mesoporous alumina	14.26	[13]
Mussel shell	141.65	[20]
A nanoparticle of wild herbs	15.75	[7]
Moroccan pyrophyllite	9.58	[5]
Banana peel	19,671	[4]

3.6 Adsorption Diffusion Mechanism

The adsorption process may be controlled by external mass transfer, intra-particle diffusion, or a combination of the two i.e. solute transfer processes [19]. The intra-particle diffusion model in Equation 19 was developed by [23].

$$q_t = k_{id}\sqrt{t} + I \ldots\ldots 19$$

Where; k_{id} is the intra-particle diffusion rate constant (mg/(g $min^{1/2}$)) and I (mg/g) is a constant that gives an idea about the thickness of the boundary layer. For the intra-particle diffusion to be the sole mechanism controlling the adsorption process, the plot of q_t against $t^{1/2}$ has to be linear passing through the origin [23]. But the plot in Figure 5 is multi-linear, indicating that the intra-particle diffusion is not the only sorption rate-controlling step [5]. It suggests that boundary layer diffusion also contributes to the uptake of EBT onto Al-beads [24]. Furthermore, the I value of 15.34, implies the thickness of the boundary is very small, hence surface diffusion plays some role in the overall adsorption process. Thus, the rate-limiting step may be a complex combination of chemisorptions and intra-particle transport [19, 23].

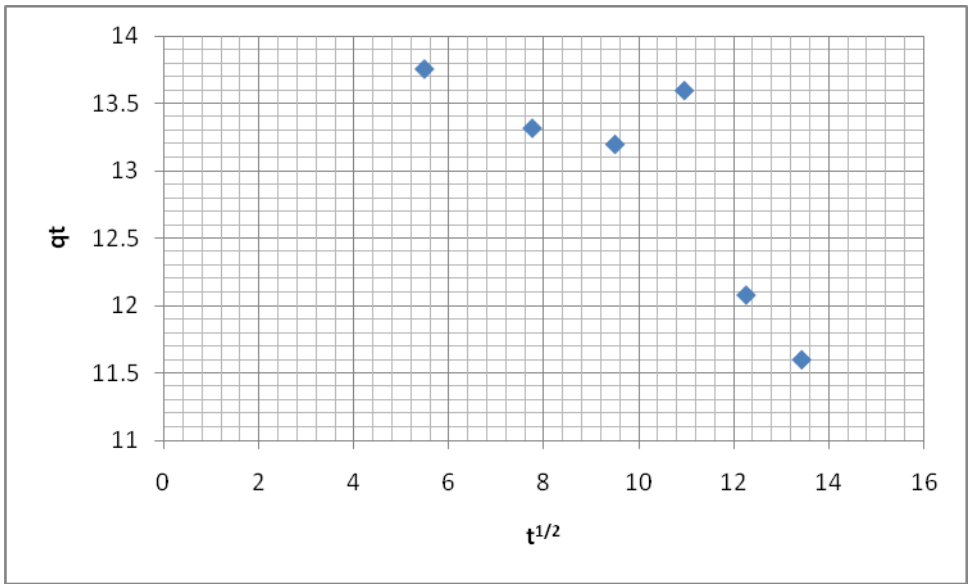

Figure 5: Intra-particle diffusion plot

The possibility of external diffusion contributing to the sorption rate-controlling step was evaluated using the model developed by [26], in Equation 20:

$$In\frac{C_t}{C_0} = -k_f\frac{A}{V}t \ldots\ldots 20$$

Where; C_0 (mg/L) is the initial dye concentration, C_t (mg/L) is the dye concentration at time t, A/V is the external adsorption area to the total solution volume, t is the adsorption time, and k_f is the external diffusion coefficient. The non-linear nature of the plot of ln C_t/C_0 versus t in Figure 6 indicated that external diffusion only contributes to the adsorption mechanism.

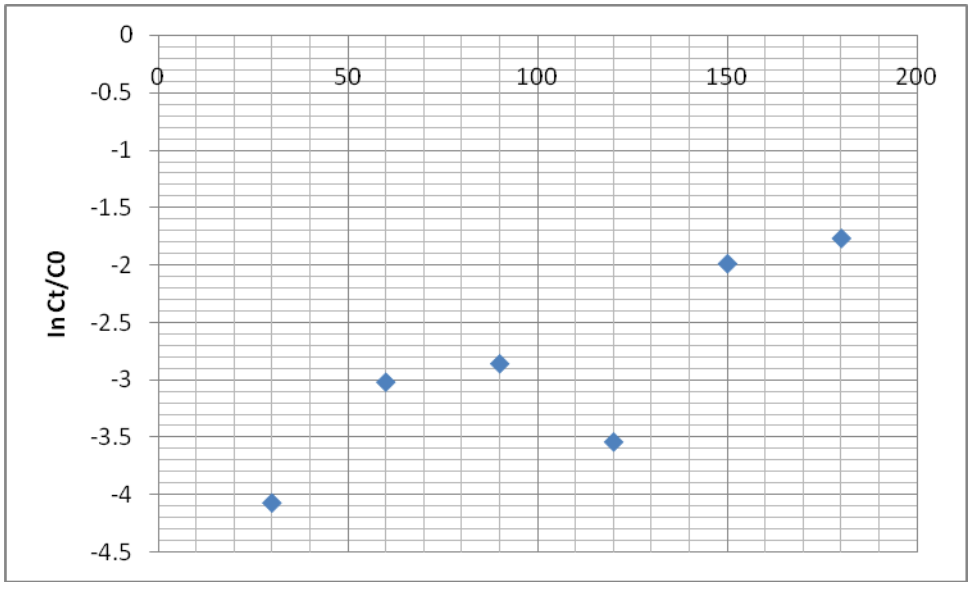

Figure 6: External diffusion plot

Conclusion

The adsorption of Eriochrome Black T dye by Al-beads was optimized by RSM analysis using Central Composite Design. From the optimization result, the most influential variables are the adsorbent dosage, initial dye concentration, the interaction between adsorbent dosage with itself, interaction of pH with itself, and that of adsorbent dosage with initial dye concentration. The R^2 value of 0.9314 implies that

93.14% of the percent dye removal could be due to the variation in the independent variable. Whereas the Adeq. precision of 13.130, and lack of fit (3.13) implies the model can be used to navigate the design space. Up to 98.28%, dye removal was attained using the Al-beads under the conditions; pH of 12.39, adsorbent dosage (1.25 g), and initial dye concentration (175 ppm). The adsorption data were fitted to Freundlich and Temkin isotherm models, while the kinetics study revealed that the pseudo-second-order model was the best fit. Furthermore, the adsorption mechanism was found to be governed majorly by intra-particle diffusion with some contribution from external mass transfer diffusion.

Acknowledgment

The authors would like to acknowledge the Tertiary Education Trust Fund (TETFund), Nigeria under Institutional Based Research (IBR) funds for the financial support provided.

Reference

[1] K. G. Akpomie and F. A. Dawodu, "Acid-modified montmorillonite for sorption of," *Beni-Suef Univ. J. Basic Appl. Sci.*, vol. 5, no. 1, pp. 1–12, 2016, doi: 10.1016/j.bjbas.2016.01.003.

[2] R. Castañeda, S. León, E. Robles-belmont, and E. Záyago, "Review of nanotechnology value chain for water treatment applications in Mexico," *Resour. Technol.*, vol. 3, no. 1, pp. 1–11, 2017, doi: 10.1016/j.reffit.2017.01.008.

[3] R. Elmoubarki, F. Z. Mahjoubi, H. Tounsadi, and J. Moustadraf, "Adsorption of textile dyes on raw and decanted Moroccan clays : Kinetics , equilibrium and thermodynamics," *Water Resour. Ind.*, vol. 9, pp. 16–29, 2015, doi: 10.1016/j.wri.2014.11.001.

[4] K. Amel, M. A. Hassena, and D. Kerroum, "Isotherm and Kinetics Study of Biosorption of Cationic Dye onto Banana Peel," vol. 19, pp. 286–295, 2012, doi: 10.1016/j.egypro.2012.05.208.

[5] Y. Miyah, A. Lahrichi, and M. Idrissi, "Assessment of adsorption kinetics for removal potential of Crystal Violet dye from aqueous solutions using Moroccan pyrophyllite," pp. 20–28, 2017, doi: 10.1016/j.jaubas.2016.06.001.

[6] A. M. Mahmoud, F. A. Ibrahim, S. A. Shaban, and N. A. Youssef, "Adsorption of heavy metal ion from aqueous solution by nickel oxide nano catalyst prepared by different methods," *Egypt. J. Pet.*, vol. 24, no. 1, pp. 27–35, 2015, doi: 10.1016/j.ejpe.2015.02.003.

[7] G. M. Al-senani and F. F. Al-fawzan, "Adsorption study of heavy metal ions from aqueous solution by nanoparticle of wild herbs," *Egypt. J. Aquat. Res.*, vol. 44, no. 3, pp. 187–194, 2018, doi: 10.1016/j.ejar.2018.07.006.

[8] E. E. Elsayed, "Natural diatomite as an effective adsorbent for heavy metals in water and wastewater treatment (a batch study)," *TITLE=Water Sci.*, vol. 32, no. 1, pp. 32–43, 2018, doi: 10.1016/j.wsj.2018.02.001.

[9] H. S. Mohamed, N. K. Soliman, D. A. Abdelrheem, A. A. Ramadan, A. H. Elghandour, and S. A. Ahmed, "Adsorption of Cd 2 D and Cr 3 D ions from aqueous solutions by using residue of Padina gymnospora waste as promising low-cost adsorbent," *Heliyon*, no. November 2018, p. e01287, 2019, doi: 10.1016/j.heliyon.2019.e01287.

[10] A. M. Bezerra, R. E. Santelli, P. E. Oliveira, S. L. Villar, and A. L. Escaleira, "Response surface methodology (RSM) as a tool for optimization in analytical chemistry," *Talanta*, vol. 76, pp. 965–977, 2008, doi: 10.1016/j.talanta.2008.05.019.

[11] A. S. Badday, A. Z. Abdullah, and K. Lee, "Optimization of biodiesel production process from Jatropha oil using supported heteropolyacid catalyst and assisted by ultrasonic energy," *Renew. Energy*, vol. 50, pp. 427–432, 2013, doi: 10.1016/j.renene.2012.07.013.

[12] W. M. Gitari, A. A. Izuagie, and J. R. Gumbo, "Synthesis , characterization and batch assessment of groundwater fluoride removal capacity of trimetal Mg / Ce / Mn oxide-modified diatomaceous earth," *Arab. J. Chem.*, vol. 13, no. 1, pp. 1–16, 2020, doi: 10.1016/j.arabjc.2017.01.002.

[13] G. Lee, C. Chen, S. Yang, and W. Ahn, "Enhanced adsorptive removal of fluoride using mesoporous alumina," *Microporous Mesoporous Mater.*, vol. 127, no. 1–2, pp. 152–156, 2010, doi: 10.1016/j.micromeso.2009.07.007.

[14] V. Temkin, M.J. and Pyzhev, "Recent modifications to Langmuir isotherms.," *Acta Physiochim. USSR*, vol. 12, p. 217, 1940.

[15] B. Zhao, W. Xiao, Y. Shang, H. Zhu, and R. Han, "Adsorption of light green anionic dye using cationic surfactant-modified peanut husk in batch mode," *Arab. J. Chem.*, vol. 10, pp. S3595–S3602, 2017, doi: 10.1016/j.arabjc.2014.03.010.

[16] H. Panda, N. Tiadi, M. Mohanty, and C. R. Mohanty, "Studies on adsorption behavior of an industrial waste for removal of chromium from aqueous solution," *South African J. Chem. Eng.*, vol. 23, pp. 132–138, 2017, doi: 10.1016/j.sajce.2017.05.002.

[17] M. Karnib, A. Kabbani, H. Holail, and Z. Olama, "Heavy Metals Removal Using Activated Carbon , Silica and Silica Activated Carbon Composite," *Energy Procedia*, vol. 50, pp. 113–120, 2014, doi: 10.1016/j.egypro.2014.06.014.

[18] Z. Kariuki, J. Kiptoo, and D. Onyancha, "Biosorption studies of lead and copper using rogers mushroom biomass ' Lepiota hystrix ,'" *South African J. Chem. Eng.*, vol. 23, pp. 62–70, 2017, doi: 10.1016/j.sajce.2017.02.001.

[19] S. Banerjee and M. C. Chattopadhyaya, "Adsorption characteristics for the removal of a toxic dye , tartrazine from aqueous solutions by a low cost agricultural by-product," *Arab. J. Chem.*, vol. 10, pp. S1629–S1638, 2017, doi: 10.1016/j.arabjc.2013.06.005.

[20] M. El Haddad, "Removal of Basic Fuchsin dye from water using mussel shell biomass waste as an adsorbent : Equilibrium, kinetics, and thermodynamics," *Integr. Med. Res.*, vol. 10, no. 5, pp. 664–674, 2016, doi: 10.1016/j.jtusci.2015.08.007.

[21] M. O. Dawodu and K. G. Akpomie, "Evaluating the potential of a Nigerian soil as an adsorbent for tartrazine dye: Isotherm, kinetic and thermodynamic studies," *Alexandria Eng. J.*, vol. 55, no. 4, pp. 3211–3218, 2016, doi: 10.1016/j.aej.2016.08.008.

[22] K. Okiel and M. El-sayed, "Treatment of oil – water emulsions by adsorption onto activated carbon , bentonite and deposited carbon," *Egypt. J. Pet.*, vol. 20, no. 2, pp. 9–15, 2011, doi: 10.1016/j.ejpe.2011.06.002.

[23] J. C. Weber Jr., W.J., Morris, "Kinetics of adsorption on carbon from solution.," *J. Sanit. Eng. Div. Proc. Am. Soc. Civ. Eng.*, vol. 89, p. 31, 1963.

[24] A. A. Inyinbor, F. A. Adekola, and G. A. Olatunji, "Kinetics , isotherms and thermodynamic modeling of liquid phase adsorption of Rhodamine B dye onto Raphia hookerie fruit epicarp," *Water Resour. Ind.*, vol. 15, pp. 14–27, 2016, doi: 10.1016/j.wri.2016.06.001.

[25] I. Nadir, Y. Achour, A. El Kassimi, M. El Himri, M. R. Laamari, and M. El Haddad, "Removal of Antibiotic Sulfamethazine from Aqueous Media Using Watermelon Seeds as a New Low Cost and Ecofriendly Adsorbent," *Phys. Chem. Res.*, vol. 9, no. 2, pp. 165–180, 2021, doi: 10.22036/pcr.2020.249992.1839.

[26] S. L. Lee, C.K., Low, K.S., Chew, "Removal of anion dyes by water hyacinth roots.," *Adv. Environ. Res.*, vol. 3, pp. 343–351, 1999.